PHASE TRANSFORMATIONS INVOLVING RESIDUAL STRESSES DURING GASEOUS NITRIDING OF STEEL

S. Jegou[1,2], R. Kubler[1], L. Barrallier[1], F. Roch2

[1]*MecaSurf Laboratory, Arts & Metiers ParisTech, Aix-en-Provence, France*
[2]*Aubert & Duval, ERAMET Group*

ABSTRACT

Nitriding of steels is an important treatment in duplex hardening methods. This treatment is known in the art but some advances still need to be done in terms of residual stress understanding. Although residual stresses originate from volume micro-loading accompanying the precipitation of nitrides, questions about their in-depth distribution of a nitrided layer during the treatment are still a challenge. A chemico-thermo-micromechanical model has been developed on the volume change computation of secondary phase transformation. Supported by some experimental observations (TEM, X-ray analysis, Electron Probe Micro Analysis (EPMA), ...), this model gives some better understanding about nitriding. Residual stresses are mainly due to the precipitation of semi-coherent MN nitrides (M=Cr,V,Mo,...). Moreover carbon, often not enough considered in the literature, is shown to be of importance in the process as it involves a second type of precipitation that is the transformation of carbides $M_{23}C_6$ and M_7C_3 into incoherent nitrides. The definition of the volume change of this transformation is a critical entry data of the mechanical modelling.

INTRODUCTION

Among methods used to increase the hardness and strength of work pieces, the use of phase transformations has been still standing a non-negligible place, especially in case of huge and complex shapes as exhibited in gears and bearing components. The key-point of processes using phase transformation is the precipitation of nano-scale and semi-coherent precipitates.
Nitriding is one of these thermochemical surface treatments of steels used in duplex hardening following quenching. It is based on diffusing nitrogen through a surface in order to improve mechanical properties such as fatigue life, wear and corrosion resistances [1,2].
In such process, residual stresses originate from loading induced secondary phase transformations. They are generated by the volume change between the matrix and the newly formed precipitates as observed in case of a ferritic matrix α-Fe strengthen by MN nitrides (M=Cr,V,Mo,...) during gaseous nitriding. This volume change is attributed to differences in the specific volumes and in the thermal expansion coefficients of precipitates [2,3].
Past studies mainly dealt with binary and iron-based ferritic systems (FeCr, FeV,...) and attributed the gradient of residual stresses to the typical discontinuous microstructure in such systems [4,5]. However one must take into account the presence of carbon in complex iron-based alloys in order to be representative of industrial applications. Indeed, few tens of weight percent of carbon are enough to involve a second type of nitride precipitation that is the transformation of annealed carbides $M_{23}C_6$ and M_7C_3 into incoherent nitrides. Carbon is released in the matrix and free to diffuse backward the surface and/or into the core of the material to sites with lower chemical potential. Generally it drives cementite precipitation at grain boundaries in the diffusion layer [6,7,8].
In the first section, a model of nitriding of steels based on a volume change computation accompanying the precipitation during the treatment is presented. In the second section, the model is briefly compared to some first experimental characterisations (TEM observations, X-ray diffraction analysis). This work is essential in order to understand what happens in such a treatment where several phenomena are interacting with each other without the possibility to isolate the influence of only one, as measuring the volume change of each phase.

VOLUME CHANGE : CORE OF NITRIDING MODELING

Some numerical models [4,6,10,11] attempted to describe the nitrogen and residual stress profiles of nitrided steels but mainly in case of binary and ferritic systems. However in order to take into account the presence of carbon and so predict nitriding of a complex sample, a three-step chemico-thermo-micromechanical model has been developed based on volume change computation and scale transition methods [12,13]. The example of the 32CrMoV13 steel grade nitrided 50 h at 550°C is examined.

Thermochemical modelling

The initial conditions are the initial chemical composition of studied samples and the nitriding parameters such as time, temperature and nitriding potential K_N.
The first step of this model consists in solving Fick's second law in case of nitrogen and carbon diffusion. The 1D diffusion problem is solved using a finite difference scheme implemented in a ADA program. In order to take into account precipitation, this calculus is linked to a *Thermo-Calc©* database. Phase distributions and the chemical composition are finally the output data (Fig.1.a).
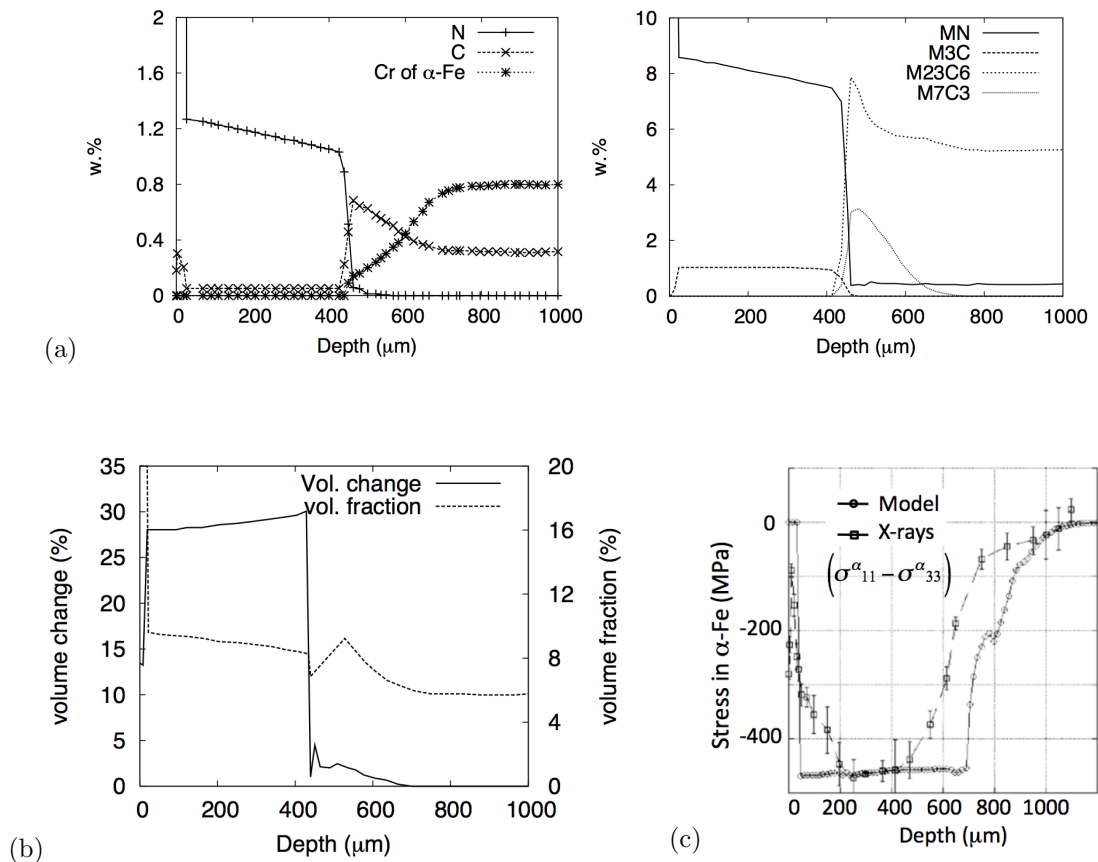

(a)

(b)

(c)

Figure 1: Example of results in case of a 32CrMoV13 steel grade nitrided 50 h at 550°C. (a) Diffusion and Precipitation prediction, (b) Corresponding Volume change and volume fraction of precipitates, (c) Residual stress profile in ferrite ($\sigma_{xx} - \sigma_{zz}$) compared to experiment (X-ray analysis)

Specific volume and volume change computation

This approach of volume change is given in line with the later self consistent scheme. In fact, whereas the volume fraction is sufficient in case of mechanical description using a simple mixture law, eigenstrain of each mechanical constituent must also be determined when using a self consistent scheme.

As residual stresses are due to volume changes accompanying the precipitation (mainly nitrides), the volumic eigenstrain of precipitates Φi has to be known, that is $\epsilon_{\Phi i}^v = \frac{1}{3}\frac{\Delta V}{V}$. The previously chemical composition due to diffusion and precipitation is used to determine the specific volume of each phase $v_{\Phi i}$, followed then by the volume change $\Delta V/V$ computation.

Specific volume and the volume of precipitates V_p are defined by :

$$v_{\Phi i} = \frac{V_{lattice} \cdot \mathcal{A}}{\displaystyle\sum_{j=1}^{q} N_{\Phi i}^{Z_j} \cdot M^{Z_j}} \quad \text{and} \quad V_p = m \cdot \sum_{i=2}^{n} v_{\Phi i} \cdot \omega_{\Phi i} \tag{1}$$

where $V_{lattice}$ is the elementary volume of lattice of phase Φi, $\mathcal{A}$ is the Avogadro's number, $N_{\Phi i}^{Z_j}$ the stoichiometric coefficient of element Z_j in phase Φi, M^{Z_j} the molar weight of element Z_j and m is the total mass of the system and $\omega_{\Phi i}$ the weight percent of phase Φi before nitriding.

In case of addition of new elements in a system such as nitrogen and even carbon, the new volume of precipitate V_p' corresponding to this new system (Fig.2) is computed assuming that heavy elements (Fe,Cr,V,...) are not diffusing during the treatment. Thus the mass increase Δm due to new atoms added at time t can be calculated based on the quantity of heavy elements at t-1 (ω^{Zj}) and t (ω'^{Zj}) as followed :

$$\Delta m = m \cdot \left(\frac{\displaystyle\sum_{j=1}^{p} \omega^{Z_j}}{\displaystyle\sum_{j=1}^{p} \omega'^{Z_j}} - 1 \right) \quad \text{and so} \quad V_p' = (m + \Delta m) \cdot \sum_{i=2}^{n} v_{\Phi i} \cdot \omega'_{\Phi i} \tag{2}$$

Finally, the volume change accompanying the precipitation is computed according two hypothesis. They express the fact that alloying elements have a high reactivity with nitrogen and suppose a complete reaction without any ferritic solid solution after the treatment.

The first one (Fig.3.) considers that iron atoms contribute to the precipitation. In other words, the total weight of iron in precipitates after nitriding ($m_p^{Fe}{}'$) is higher than before nitriding (m_p^{Fe}). The following condition and equation are so obtained :

$$\text{If } \alpha\text{-Fe} \rightarrow \text{Precipitates, or, } m_p^{Fe}{}' \geq m_p^{Fe} \text{ , then } \left.\frac{\Delta V}{V}\right|_{\mathbf{P}} = \frac{V_p'}{V_p + V_{Fe \rightarrow p}} - 1 \tag{3}$$

The second hypothesis is the opposite and suppose a dissolution of precipitates into iron :

$$\text{If Precipitates} \rightarrow \alpha\text{-Fe, or, } m_p^{Fe}{}' \leq m_p^{Fe} \text{ , then } \left.\frac{\Delta V}{V}\right|_{\mathbf{P}} = \frac{V_p' + V_{p \rightarrow Fe}}{V_p} - 1 \tag{4}$$

Where $V_{x \rightarrow y}$ is an equivalent volume of phase x transformed into phase y. An example is : $V_{Fe \rightarrow p} = (m_p^{Fe}{}' - m_p^{Fe}) \cdot v^{Fe}$.

For 32CrMoV13 steel grade after 50 h of nitriding at 550°C, the volume change profile is given in Fig.1.b. One can see that the volume change during the treatment can reach 30 % at the end of the diffusion layer that is around 450 μm. This is what is usually observed in such kind of treatment based on secondary phase transformation.
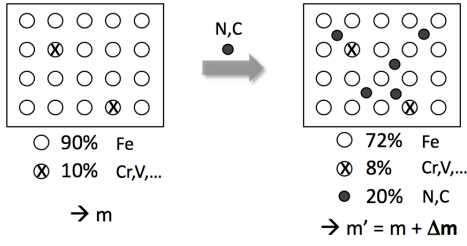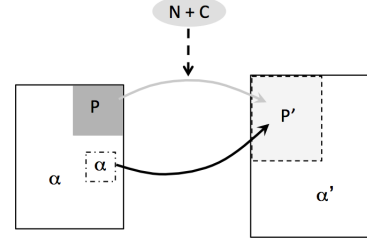
Figure 2: Addition of new elements in a system.

Figure 3: Scheme of hypothesis one in case of volume change computation.

Mechanical modelling

Since volume changes (eigenstrain) of precipitates and their respective volume fraction are known, residual stresses in each phase are computed based on an idealised microstructure of precipitated embedded in a ferritic matrix after nitriding. The use of a self-consistent scheme is adopted [14,15]. Since a local scale (phase level) and a global scale (macroscopic level) are considered, the notation for global values is $\hat{X}$. The model supposes an homogeneous and isotropic semi-infinite system in case of a small strain assumption. As observed experimentally, a nitrided surface is under a macroscopic plane stress state (Fig.4), therefore one can write :
$\forall z, \hat{\epsilon}_{xy} = \hat{\epsilon}_{yx} = 0$ and $\hat{\sigma}_{xy} = \hat{\sigma}_{yx} = 0$. Moreover, due to their nano-scale and/or semi-coherent natures, the precipitate's behaviour is assumed fully elastic : $\epsilon^p_{precipitates} = 0$.
Then constitutive equations can be written as followed depending on the considered scale :

- Macroscopic equations based on equilibrium equation and conditions on the system. Equation of strain compatibility are also used in order to take into account the in-depth gradient of strain. $\hat{\underline{\epsilon}}^l$ represents the eigenstrain tensor divided into $\hat{\underline{\epsilon}}^p$ and $\hat{\underline{\epsilon}}^v$ the plastic and volume strain respectively :

$$\begin{cases} \hat{\underline{\epsilon}} = \hat{\underline{\epsilon}}^e + \hat{\underline{\epsilon}}^l \text{ with } \hat{\underline{\epsilon}}^l = \hat{\underline{\epsilon}}^p + \hat{\underline{\epsilon}}^v \\ div \; \hat{\underline{\sigma}} = 0 \\ \hat{\epsilon}_{ij,kl} - \hat{\epsilon}_{ik,jl} = \hat{\epsilon}_{lj,ki} - \hat{\epsilon}_{lk,ji} \end{cases} \tag{5}$$

- Local equations that are phenomenological behaviour laws of ferrite and precipitates :

$$\begin{cases} \underline{\epsilon}_{\Phi i} = \underline{\epsilon}^e_{\Phi i} + \underline{\epsilon}^l_{\Phi i} \text{ with } \underline{\epsilon}^l_{\Phi i} = \underline{\epsilon}^p_{\Phi i} + \underline{\epsilon}^v_{\Phi i} \\ \underline{\sigma}_{\Phi i} = \underline{\underline{C}}_{\Phi i} : \underline{\epsilon}^e_{\Phi i} \\ \underline{\sigma}_{\alpha - Fe} = g(\underline{\epsilon}^p_{\alpha - Fe}) \end{cases} \tag{6}$$

where $\underline{\underline{C}}_{\Phi i}$ is the stiffness tensor of phase Φi, $g(\underline{\epsilon}^p_{\alpha - Fe})$ the hardening law of ferrite (Power law type) without taking into account the microstructure.

- Scale transition equations with the help of $\underline{\underline{S}}^{Esh}$ the Eshelby's tensor expressing general shape of precipitates or inclusions, $\underline{I}$ the unity tensor and $\underline{\underline{U}}$ the polarization tensor. These equations are a complex representation of common mixing laws and render heterogeneities of materials :

$$\begin{cases} \underline{\epsilon}^e = (\underline{I} + \underline{\underline{U}}) : \hat{\underline{\epsilon}}^e + (\underline{I} + \underline{\underline{U}}) : (\underline{\underline{S}}^{Esh} - \underline{I}) : (\underline{\epsilon}^l - \hat{\underline{\epsilon}}^l) \\ \hat{\underline{\sigma}} = \sum_i y_{\Phi i} \cdot \underline{\sigma}_{\Phi i} \end{cases} \tag{7}$$

Those equations are solved with an iterative Newton-Raphson scheme and implemented in a ADA program in order to output residual stresses profiles in each phase. For the case of the 32CrMoV13 steel grade after 50 h of nitriding at 550°C, the residual stress profile $(\sigma_{\Phi i,xx} - \sigma_{\Phi i,zz})$ vs. depth in ferrite is compared to experimental X ray stress profile as seen on Fig.1.c.

Example and Discussion

Figure 1 gives an example in case of nitriding of a 32CrMoV13 steel grade at 550°C during 50 h. Concerning residual stresses in ferrite, both the maximum of stress and the width of stress profile are in good agreements with those from an experimental profile obtained by X-ray analysis and the $sin^2\Psi$ method (Fig.1.c). However some discrepancies exist about the distribution of stresses in depth of the nitrided layer : a flat profile has to be compared to a curved one.
That must be explained first by no considerations on microstructure, especially ferrite strengthen by semi-coherent nitrites. In fact, the elastoplastic behaviour of a nitrided sample can be described using a Swift law [16] but it depends usually on depth and therefore on nitrogen and carbon diffusion, time and temperature of the treatment and also on the initial chemical composition. Moreover, models describing interactions between precipitates (such as Mori-Tanaka scheme) have not been introduced in the model yet but are also in consideration.

EXPERIMENTAL DATASET

Materials investigated in this study are taken from a set of three laboratory samples : two ternary steels (Fe-0,37%C-1%Cr and Fe-0,35%C-3%Cr) and one quaternary sample (Fe-0,38%C-1%Cr-0,2%Al). The industrial 32CrMoV13 steel grade was also used. All were manufactured by Aubert & Duval (heated, quenched and annealed) and also nitrided in a 500-550°C temperature range and treatment times were 50 or 100 hours. All other parameters for samples elaboration stay confidential.
Transmission Electron Microscopy (TEM) observations were performed on JEOL JEM 2010F URP22. Sample preparations were done using a Philips FIB 200 TEM Focused Ion Beam.

EXPERIMENTAL CHARACTERIZATIONS

Volume fraction of MN nitrides

In this section, the experimental determination of the quantity of nitrides, the main secondary phase during nitriding is adressed. Comparisons between experimental (showed by stars on Fig.4 and 5) and predicted values of the volume fraction of nitrides are made. The case of a 32CrMoV13 steel grade nitrided 50h (Fig.4.) and 100h (Fig.5.) at 550°C is investigated. Experimental observations are taken from a TEM study of Locquet [7]. The nitrided depths are respectively 450 and 650 μm. Nitrogen and carbon profiles on Fig.6 were obtained by EPMA analysis.
Comparing nitrogen profiles from Fig.4 and Fig.5 shows that the diffusion of nitrogen is accurately predicted by Fick's second law linked to a Thermo-Calc database. However the predicted volume fraction of nitrides is overestimated in comparison to experimentation (Fig.4). Injecting experimental nitrogen and carbon profiles in the model gives good agreements in terms of thermodynamical prediction as shown in Fig.5. Moreover the only difference is the carbon profile. It is noticeable that the predicted carbon diffusion does not correspond to the reality between 20 and 450 μm on Fig.4, but the model is able to detect decarburizing and especially the carbon enrichment at the end of the diffusion layer. Therefore nitriding involves a complex redistribution of carbon in depth of a surface and a carbon diffusion kinetic is needed. It has to take into account either a diffusion into the core of the material and/or a decarburizing phenomenon.

Furthermore, it has to be noticed on Fig.5 that the model predicts mainly the precipitation of complex nitrides MN where M can be chromium, vanadium, molybdenum and even iron up to 15 at.%. This result is in correlation with the chemical composition of nitrides found by Ginter [8], suggesting that nitriding uptake in a nitrided layer can be explained by a substitution of alloying elements with iron atoms.
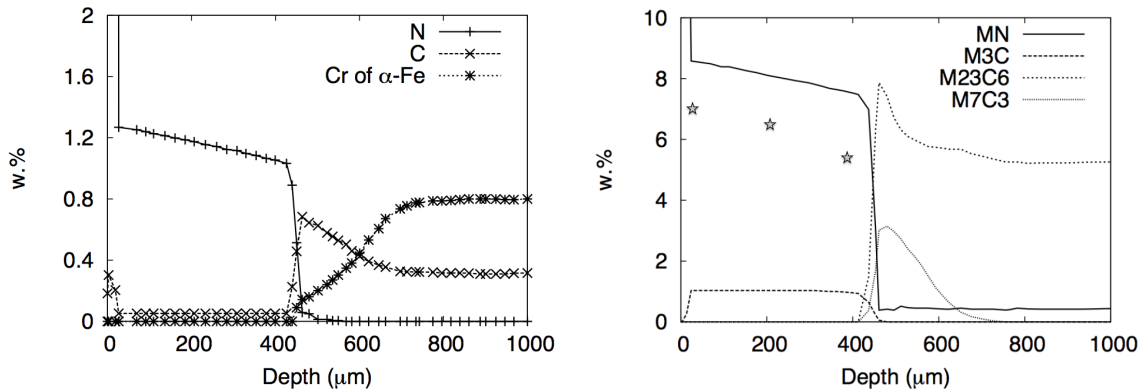
Figure 4: Comparisons between modelling and experimental data (stars) [7] using diffusion simulations in case of a 32CrMoV13 steel grade nitrided 50 h at 550°C.
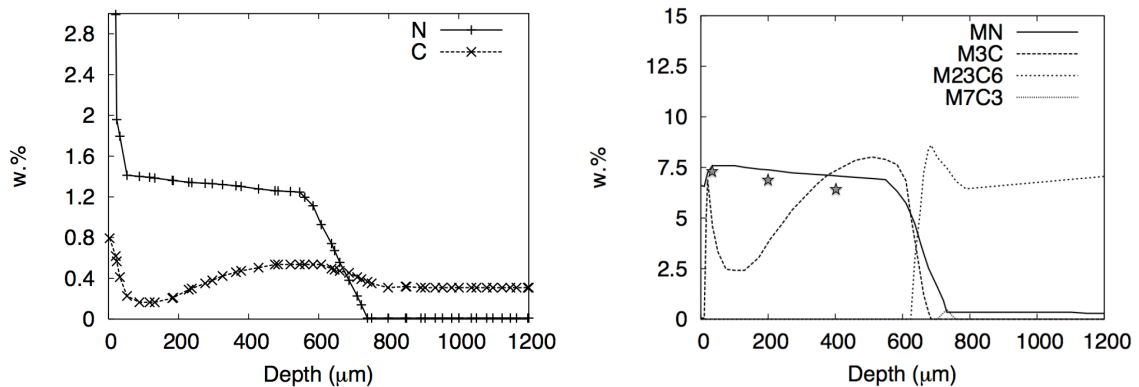

Figure 5: Comparisons between model and experimental data (stars) [7] using experimental nitrogen and carbon profiles in case of a 32CrMoV13 steel grade nitrided 100 h at 550°C.

Carbon enrichment near the end of the diffusion layer

The last experimental characterisation is about consequences due to carbon diffusion into the core of the material. A carbon enrichment is usually found at the end of the nitrided layer (see Fig.5 at 600 μm). The figure 6 represents a nitrogen profile (EPMA analysis) where the depth of the diffusion front is about 850 μm in case of Fe-0,35%C-3%Cr nitrided 100 h at 550°C. The depth of possible carbon enrichment is also reported and is 920 μm.

If a carbon enrichment is observed at the end of the diffusion layer where just few nitrogen atoms exist, two hypothesis can be made : either the density of carbides increases and/or the size of carbides increases by a depletion of alloying elements from the ferritic solid solution. These are in good agreements with the model. On Fig.4, the quantity of chromium in ferrite is reported. At the end of the diffusion layer, a depletion of chromium is found due to an increase of the carbides quantity following a carbon enrichment.

TEM observations (Fig.7) were performed to look at these information, and especially the size of carbides. The two charts of Fig.8 present the distribution of size of carbides corresponding to the core of the material and to 920 μm. The population corresponding to the core of the material still exists at 920 μm, but smaller precipitates (30-60 μm) exhibit growth during nitriding to a 80-160 μm range. The hypothesis that the size of carbides increases following a carbon enrichment at the end of the diffusion layer is verified.
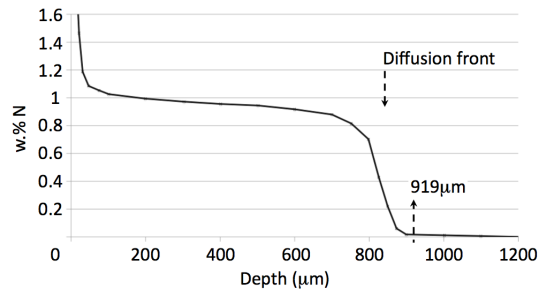
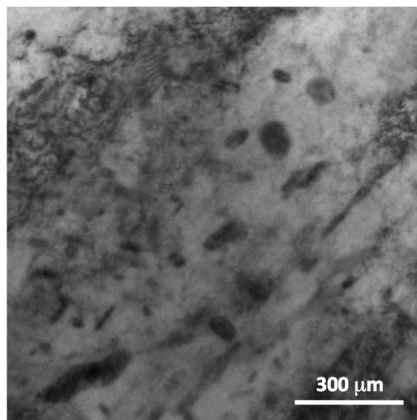Figure 6: EPMA nitrogen profile of Fe-0,35%C-3%Cr nitrided 100 h at 550°C.

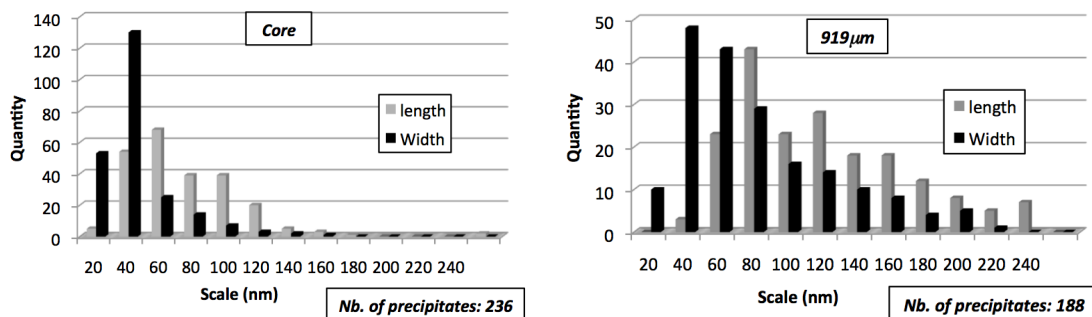Figure 7: TEM micrography from the core of Fe-0,35%C-3%Cr nitrided 100 h at 550°C.

Figure 8: Size of carbides distribution corresponding to the core of the material and to the depth of carbon enrichiment. Fe-0,35%C-3%Cr nitrided 100 h at 550°C.

CONCLUSION

A model of nitriding was presented taking into account diffusion, precipitation and multi-scale mechanical descriptions. It is based on the volume change computation accompanying the precipitation. It represents a powerful tool in order to understand the microstructural evolution as well as the generation of residual stresses.

Some experimental characterisations were presented that are in correlations with the model. In case of complex iron-based alloys, carbon is of importance since it induces a second type of

nitrides precipitation and then diffuses in parallel to nitrogen. The results are complex chemical and thermodynamical changes in the nitrided layer and in the next beneath region.

The main transformation involving residual stresses during nitriding is the transformation of a volume of ferrite into a volume of nitrides. Correlations between our model and experimental observations suggest also a non negligible role played by the transformation of carbides into incoherent nitrides on stress (re-)distribution depending on depth and time. Carbon diffusion kinetic and details about the transformation of carbides into nitrides are needed in order to develop a better volume change computation method.

Stress (re-)distribution during the treatment is the consequence of complex interactions between thermodynamical and mechanical phenomena. The role of the size of precipitates is also under consideration in order to take into account the microstructure in the hardening law of ferrite.

Acknowledgment

REFERENCES

[1]   E.J. Mittemeijer, Mater Sci Forum, **223** (1992) 102-104.

[2]   F. Ashrafizadeh, "Influence of plasma and gas nitriding on fatigue resistance of plain carbon (ck45) steel", Surface and Coatings Technology, **173-174** (2003) 1196-1200.

[3]   L. Barrallier and J. Barrallis, "On origin of residual stresses generated by nitriding treatment on alloy steels", Proceedings of ICRS4 (1994) 498-505.

[4]   H. Oettel and G. Schreiber, "Nitrieren und Nitrocarburieren", AWT-Tagungsband, AWT, Wiesbaden, Germany (1991) 139-151.

[5]   N.E. Vives Diaz, R.E. Schacherl, L.F. Zagonel and E.J. Mittemeijer, "Influence of the microstructure on the residual stresses on nitrided iron-chromium alloys", Acta Materialia, **56** (2008) 1196-1208.

[6]   M.A.J. Somers, "Modelling nitriding of iron : from thermodynamics to residual stress", Journal de Physique IV, **120** (2004) 21-33.

[7]   J.N. Locquet, Phd Thesis, Arts & Metiers - ParisTech, France (1998).

[8]   C. Ginter, L. Torchane, J. Dulcy, M. Gantois, A. Malchere, C. Esnouf and T. Turpin, "A new approach to hardening mechanisms in the diffusion layer of gas nitrided α-alloyed steels. Effects of chromium and aluminium : experimental and simulation studies", La Metallurgia Italiana, **7-8** (2006) 29-35.

[9]   V.Y. Traskine, S.E. Bochenkov and L. Barrallier, "Physicochemical Mechanics of Structural Transformations in Nitrided Steel", Colloid Journal, **67** (2005) 106-112.

[10]   S.S. Hosmani, R.E. Schacherl and E.J. Mittemeijer, "Kinetics of nitriding Fe-2 wt Pct V Alloy : Mobile and Immobile Excess Nitrogen", Metallurgical and Materials Transactions A, **38A** (2007) 7-16.

[11]   V. Leskovsek, B. Podgornik and D. Nolan, "Modelling of residual stress profiles in plasma nitrided tool steel", Materials Characterisation, **59** (2008) 454-461.

[12]   L. Barrallier, Phd Thesis, Arts & Metiers - ParisTech, France (1992).

[13]   V. Goret, Phd Thesis, Arts & Metiers - ParisTech, France (2006).

[14]   D. François, A. Pineau and A. Zaoui, "Comportement mécanique des matériaux", Hermés, France (1991).

[15]   T. Mura, "Micromechanics of Defects in Solids", Kluwer Academic Publishers, 2nd Edition (1991).

[16]   C. Jacq, G. Lormand, D. Nelias, D. Girodin and A. Vincent, "On the influence of residual stresses in determining the micro-yield stress profile in a nitrided steel by nano-indentation", Materials Science and Engineering A, **342** (2003) 311-319.